ACS OMEGA

Open Access

http://pubs.acs.org/journal/acsodf

Article

Design and Synthesis of Novel Thieno[3,2-*c*]quinoline Compounds with Antiproliferative Activity on RET-Dependent Medullary Thyroid Cancer Cells

Gabriele La Monica, Giuseppe Pizzolanti, Concetta Baiamonte, Alessia Bono, Federica Alamia, Francesco Mingoia, Antonino Lauria, and Annamaria Martorana*

Cite This: *ACS Omega* 2023, 8, 34640−34649

Read Online

ACCESS | Metrics & More | Article Recommendations | Supporting Information

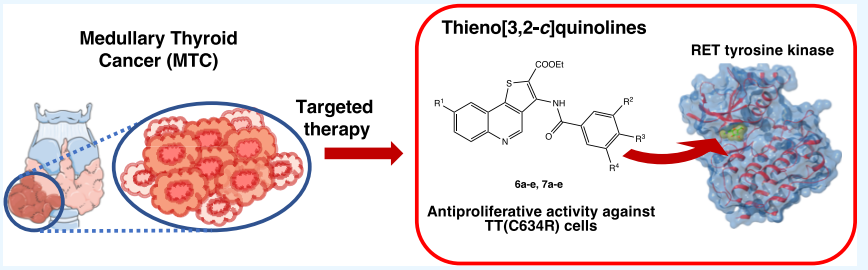

ABSTRACT: RET kinase gain-of-function mutations represent the main cause of the high aggressiveness and invasiveness of medullary thyroid cancer (MTC). The selective inhibition of the RET kinase is a suitable strategy for the treatment of this endocrine neoplasia. Herein, we performed an innovative ligand-based virtual screening protocol using the DRUDIT^{online} web service, focusing on the RET kinase as a biological target. In this process, thieno[3,2-*c*]quinolines **6a−e** and **7a−e** were proposed as new potential RET inhibitors. The selected compounds were synthetized by appropriate synthetic strategies, and *in vitro* evaluation of antiproliferative properties conducted on the particularly aggressive MTC cell line TT(C634R) identified compounds **6a−d** as promising anticancer agents, with IC_{50} values in the micromolar range. Further structure-based computational studies revealed a significant capability of the most active compounds to the complex RET tyrosine kinase domain. The interesting antiproliferative results supported by *in silico* predictions suggest that these compounds may represent a starting point for the development of a new series of small heterocyclic molecules for the treatment of MTC.

1. INTRODUCTION

Thyroid cancer is a heterogeneous type of cancer, whose incidence has increased in recent years. It represents a benchmark in the development of oncologic therapies for the treatment of solid tumors, as its progression involves potential druggable targets. From a histological point of view, thyroid cancer can be classified in three main subtypes: differentiated thyroid cancer (DTC), anaplastic thyroid cancer (ATC), and medullary thyroid cancer (MTC). MTC arises from parafollicular C cells, involved in the production and release of calcitonin, and can be either familial [the multiple endocrine neoplasia syndromes types 2A and 2B (MEN2A and MEN2B), in 25% of patients] or sporadic (in 75% of patients).[1,2] Currently, genetic analyses aimed at directly improving a patient response to treatment, identifying the RET (rearranged during transfection) gene point mutations as the major responsible for the occurrence of MTC.[3,4] RET, a key proto-oncogene on human chromosome 10q11.21, encodes a tyrosine kinase receptor (RTK) essential for the normal development of the brain, the peripheral sympathetic and parasympathetic nervous systems, the regulation of cell migration, differentiation, and proliferation. Structurally, the RET receptor consists of 1114 amino acids and three domains: the extracellular, the hydrophobic transmembrane, and the intracellular tyrosine kinase domains. The extracellular domain comprises 636 residues and is subdivided into four cadherin-like regions (CLD1−4), with approximately 110 residues each, a cysteine-rich domain (CRD) with 120 residues, and the Ca^{2+} binding site in the region between CLD2 and CLD3. The intracellular domain is characterized by a juxta-membrane domain of 50 residues, two tyrosine kinase domains, and a C-terminal tail (Figure 1a).[5,6] Seven disulfide bonds are located in the CRD and another one in the linker region between the CRD and the transmembrane domain. As a result of an alternative splicing mechanism, three RET protein isoforms

Received: May 22, 2023
Accepted: July 25, 2023
Published: September 11, 2023

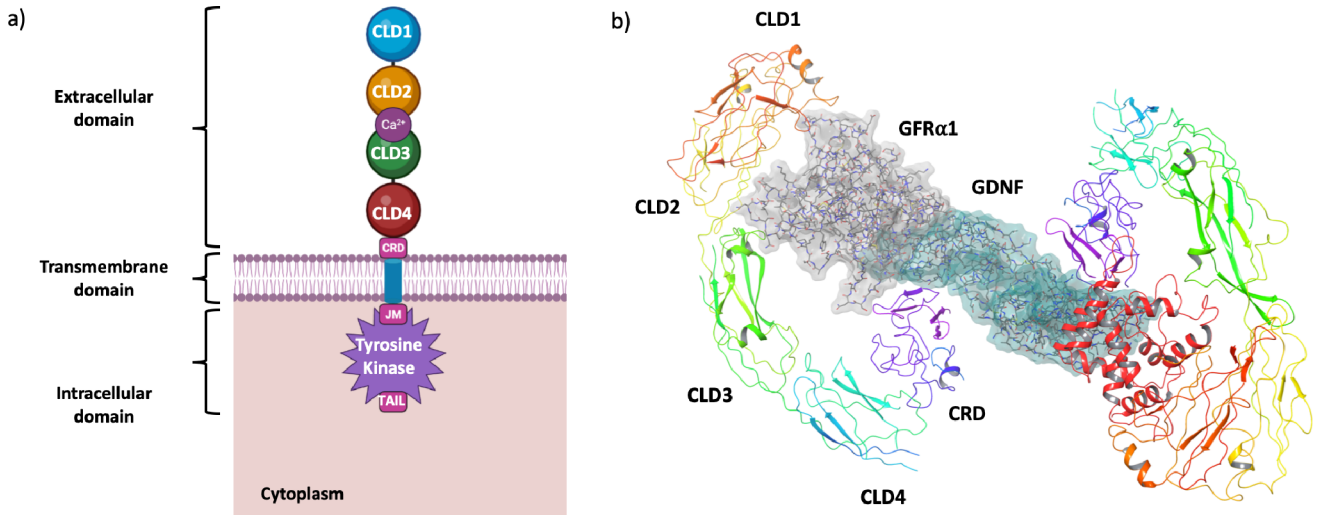

Figure 1. (a) 2D representation of the three domains of the receptor tyrosine kinase RET; (b) structure of the RET/GFRα1/GDNF complex based on the PDB code 6Q2N.

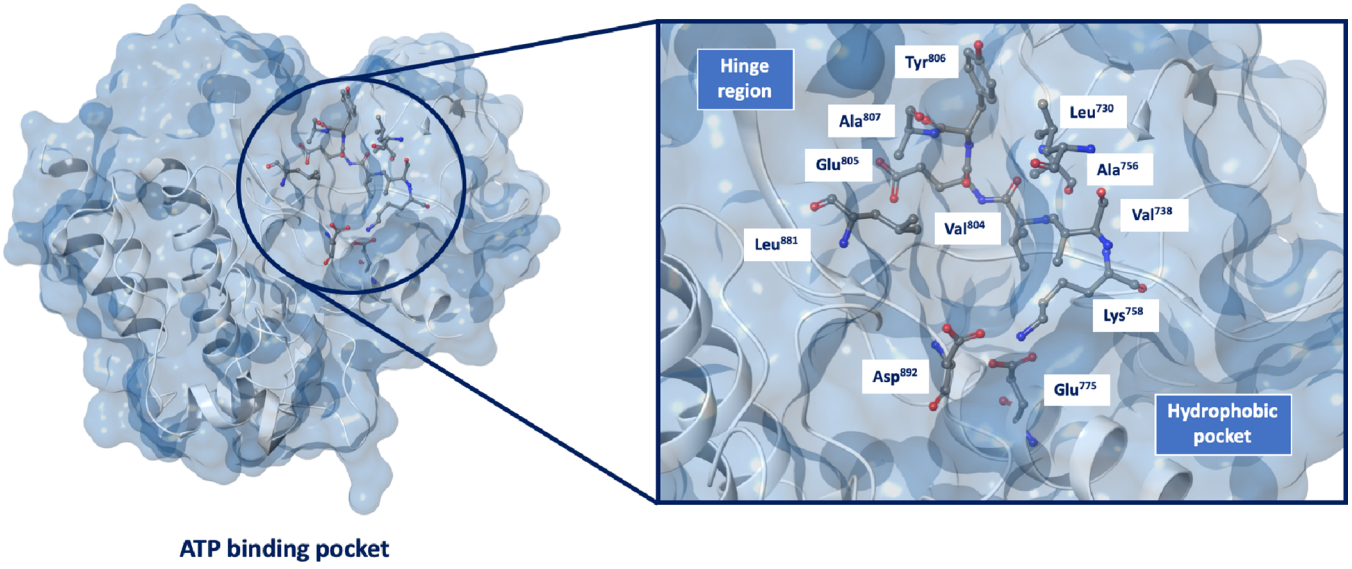

Figure 2. X-ray structure of the RET ATP binding site, focusing on the hinge region, the hydrophobic pocket, and the amino acid residues involved (PDB code: 6NEC).

exist, differing in the amino acid sequence at the C-terminal tail: the short (RET9), the intermediate (RET43), and the long isoform (RET51). RET9 and RET51 are ubiquitous, and RET43 is found only in primates and some lower species.[6,7] The process of RET protein kinase activation requires the formation of a preliminary binary complex between the glial cell line-derived neurotrophic factor (GDNF) family ligands and the GDNF family co-receptors (GFRα1−4). Subsequently, RET dimerization is induced by binding to the binary complex, to form a ternary complex, that turned on the kinase receptor (Figure 1b).[8] Dimerization of RET and its activation cause a conformational change of the receptor, leading to the trans-autophosphorylation of specific tyrosine residues in the intracellular tyrosine kinase domain (Tyr^{900}, Tyr^{905}, Tyr^{1062}, and Tyr^{1096}). Phosphorylated tyrosine residues are important sites for several adaptor proteins, which play key roles in the process of intracellular signal transduction through a plethora of pathways.[9,10]

To date, 100 mutations have been described in the RET gene. In particular, cancers associated with RET are usually gain-of-function mutations in this protein, affecting the cysteine-rich ($Cys^{634}Arg$ in patients with MEN2A) or tyrosine kinase domains ($Leu^{790}Phe$, $Tyr^{791}Phe$, $Ser^{891}Ala$, and $Arg^{844}Leu$ in patients with MTC and MEN2A; $Met^{918}Thr$ in 95% of MEN2B patients). The resulting mutant protein leads to constitutive receptor dimerization and aberrant signal transduction.[4,11,12] RET point mutations are a major cause of the familial frequency of MTC, MEN2A, and MEN2B, making this kinase receptor a distinctive therapeutic target for a targeted treatment of thyroid cancers.[13]

Due to the similarity of the RET binding site with other RTKs, several multikinase inhibitors (MKIs), such as *vandetanib*,[14] *cabozantinib*,[15] *lenvatinib*,[16] *sorafenib*,[17] and *nintedanib*,[14] have shown promising RET inhibitory activity,[18] although their use is currently limited by the high dose required.

https://doi.org/10.1021/acsomega.3c03578
ACS Omega 2023, 8, 34640−34649

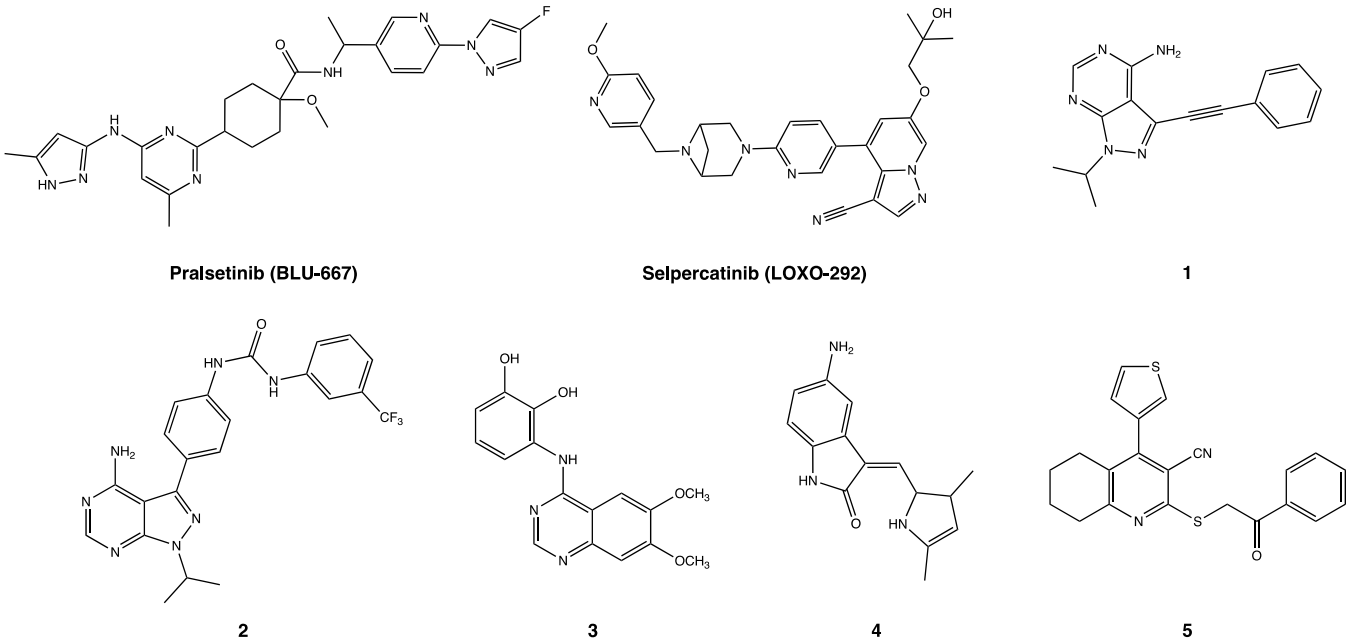

Figure 3. 2D chemical structures of RET inhibitors **1**−**5** and the recently FDA-approved selective RET inhibitors *pralsetinib* and *selpercatinib*.

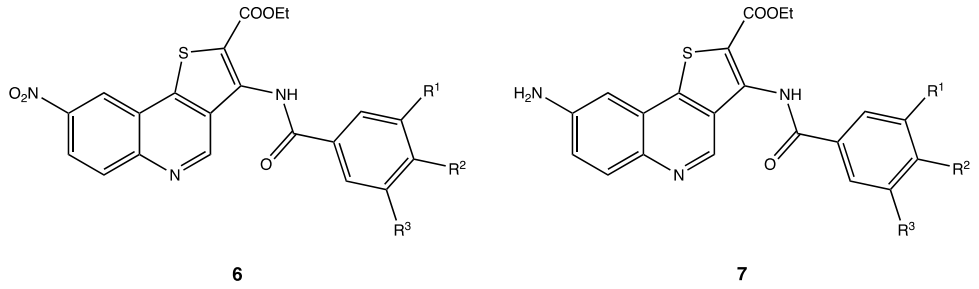

Figure 4. Chemical structures of the under-investigated thieno[3,2-*c*]quinoline compounds of types **6** and **7**.

With the aim of circumventing the acquired resistance to MKIs and the toxic effects due to their promiscuous off-target activities, the selective inhibitors of RET represent therefore a focus of research. In general, they should meet basic structural requirements: a hinge binding moiety (usually consisting of a heterocyclic core) that acts as a hydrogen bond donor or acceptor to interact with the key residues Ala^{807} and/or Glu^{805} in the hinge region and a hydrophobic group that fits into the hydrophobic pocket of the ATP binding site (Leu^{730}, Val^{738}, Ala^{756}, Lys^{758}, Glu^{775}, and Asp^{892}). Furthermore, from a structural point of view, the gatekeeper residue Val^{804} is important to control the access of small molecules to a hydrophobic cavity. Indeed, the Val^{804}Met and Val^{804}Leu mutations lead to drug resistance (Figure 2).

In 2020, the two RET-selective inhibitors *pralsetinib* (BLU-667) and *selpercatinib* (LOXO-292) were approved by the FDA for the treatment of RET-driven or thyroid cancer (Figure 3).[19−21] Although they represented a turning point in the targeted therapy for these malignancies (higher efficacy, selectivity, more favorable pharmacokinetic properties, and fewer off-target interactions compared with the aforementioned MKIs), the development of resistance due to RET point mutations (e.g., Gly^{810}Arg/Ser/Cys/Val, Leu^{730}Val/Iso, and Tyr^{806}Cys/Asn) also began to occur early with these drugs.[21−23]

For these reasons, in the last decades, many other aromatic scaffolds have been investigated in the design of new potential selective RET inhibitors for their capability to deeply penetrate the hinge region of the kinase.[7] Among them, pyrazolopyrimidine,[24−28] quinazoline,[12,29−33] indolinone,[34] nicotinonitrile,[35] pyridone,[36] 1,2,4-triazole,[37] and pyrazolo[1,5-*a*]-pyridine[26] are worth mentioning, and as examples, derivatives **1**−**5** with significant inhibitory activity against the RET kinase (IC_{50} values of 8 nM, 2 nM, 3.9 nM, 0.3 μM, and 2.3 μM, respectively) are shown in Figure 3.

2. RESULTS AND DISCUSSION

In view of these considerations and with the goal of discovering new agents for the treatment of RET-altered thyroid cancer, in this work, we applied our experience in *in silico* virtual screenings[38−45] to evaluate a large structural database. In particular, we performed a virtual screening to assess the affinity of an in-house structural database (about 10,000 heterocyclic compounds) for the RET kinase as a focused biological target.

For this purpose, the DRUDIT BIOTARGET^{finder} protocol, a ligand-based tool capable of predicting the affinity of input structures against the target(s) of interest, was used.[46] This tool is based on molecular descriptor calculation and is able to assign an affinity score (DAS, DRUDIT Affinity Score, in the range of 0−1) to each input structure against the target(s) of

https://doi.org/10.1021/acsomega.3c03578
ACS Omega 2023, 8, 34640−34649

interest. The DRUDIT molecular descriptor-based template of RET was built from known RET inhibitors reported in the literature and implemented in the DRUDIT[online] web platform (https://www.drudit.com/).[46]

The analysis of the *in silico* results highlights the compounds of types **6a−e** and **7a−e** (Figure 4 and Table 1), with a polycondensed tricyclic thieno[3,2-*c*]quinoline scaffold, as the best ranked structures against the RET kinase.

Table 1. DRUDIT Affinity Score (DAS) Values for the Thieno[3,2-*c*]quinoline of Type 6a−e and 7a−e and Reference Compounds

compound	R^1	R^2	R^3	DAS (RET kinase)
6a	H	H	H	0.84
6b	H	CH_3	H	0.84
6c	H	OCH_3	H	0.85
6d	H	CF_3	H	0.78
6e	Cl	F	H	0.75
7a	H	H	H	0.89
7b	H	CH_3	H	0.89
7c	H	OCH_3	H	0.89
7d	H	CF_3	H	0.80
7e	Cl	F	H	0.82
nintedanib				0.95
vandetanib				0.85

In this regard, several published papers attribute antiproliferative biological activity to the quinoline/quinazoline scaffold, which constitutes the central core even in many RET inhibitors approved in therapy (*vandetanib*, *cabozantinib*, and *lenvatinib*).[3,14,29,30,47−50]

As shown in Table 1, the DAS values in the range of 0.75−0.89 are comparable to the already approved RET kinase inhibitors *vandetanib* and *nintedanib* (DAS values of 0.85 and 0.95, respectively).

In terms of structural similarity, the thienoquinoline compounds meet the general requirements presented by the RET quinoline/quinazoline inhibitors mentioned above. The tricyclic thienoquinoline ring system could correspond to the central pharmacophoric aromatic core, with donor and/or acceptor hydrogen bond groups, and the hydrophobic aromatic side ring could fit into the hydrophobic pocket of the RET ATP binding site.

Thus, based on the encouraging *in silico* results, we decided to synthetize the selected quinoline compounds, establishing appropriate synthetic strategies.

The overall synthetic pathway for the preparation of 3-benzoylamino-thieno[3,2-*c*]quinoline derivatives **6a−e** and **7a−e** involves six steps, starting from the commercially available 4-nitroaniline (**8**) (Scheme 1). The intermediates **9−11** were obtained following the procedure reported in the literature.[51] The next synthetic step involves the isolation of the thieno[3,2-*c*]quinoline core **12**, the polycondensed aromatic thienoquinoline system. The presence of both cyano and nitro substituents on quinoline nucleus **11** enhanced the reactivity of the chlorine atom, which readily underwent nucleophilic displacement by ethyl thioglycolate, in the presence of triethylamine as the base and dimethyl sulfoxide (DMSO) as the solvent. The consequent *in situ* intramolecular cyclization allowed to the formation of the thienoquinoline system and therefore the isolation of derivative **12** in quantitative yields. To introduce the benzoyl moiety, amino derivative **12** was treated with substituted benzoyl chlorides. The nucleophilic acyl substitution was carried out under strictly anhydrous conditions, employing a DMAP/pyridine mixture as the base and DCM as the solvent. The use of these reaction media significantly shortened the reaction time, leading to derivatives **6a−e** at room temperature in 12 h. Finally, reduction of the nitro group on compounds **6a−e** was realized by hydrogenation with 10% Pd/C in ethanol. After removal of the catalyst, amino derivatives **7a−e** were easily isolated as pure needles in good/excellent yields (48−95%).

The anticancer activity of all the synthetized compounds **6a−e** and **7a−e** was evaluated, using the MTT assay, against the particularly aggressive MTC cell line TT(C634R), harboring a pathogenic mutation in the cysteine-rich domain of the RET kinase. Among all, nitro compounds **6a−d** exhibited interesting antiproliferative activity. IC_{50} was calculated using the GraphPad software after approximately

Scheme 1. Synthesis of Derivatives 6a−e and 7a−e[a]

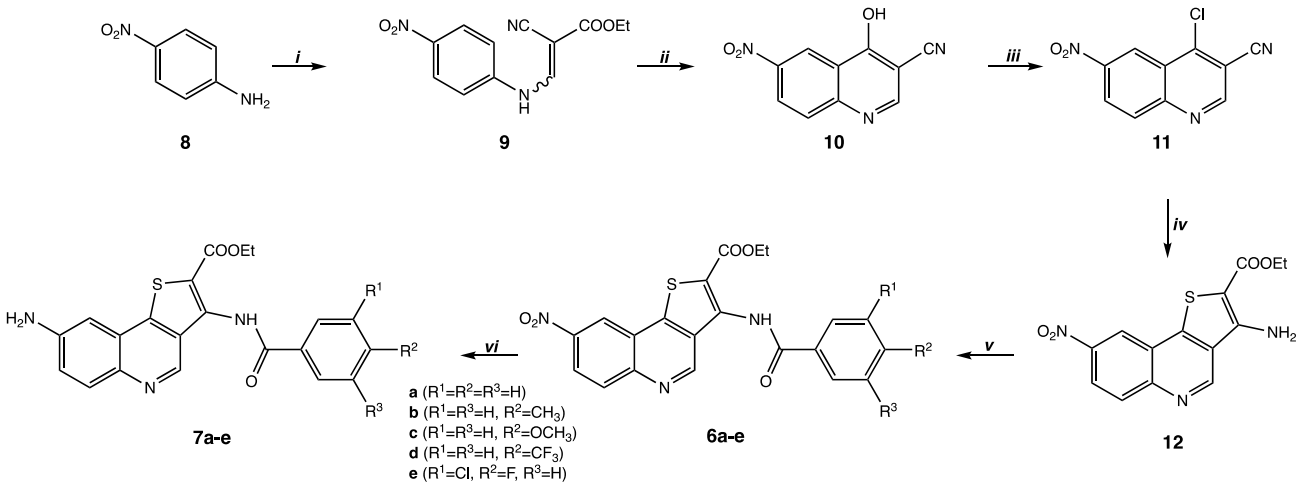

[a]Reagents and conditions: (i) ethyl-2-cyano-3-ethoxyacrylate, toluene, reflux 12 h; (ii) Dowtherm A, N_2, reflux, 10 h; (iii) $POCl_3$, reflux, 8 h; (iv) ethyl thioglycolate, NEt_3, dry DMSO, rt 2 h; (v) appropriate benzoyl chloride (4 equiv), pyridine/DMAP (2:2 equiv), dry DCM, rt 12−24 h; (vi) 10% Pd/C, H_2, ethanol, rt 24 h.

https://doi.org/10.1021/acsomega.3c03578
ACS Omega 2023, 8, 34640−34649

one and two doubling times (3 and 6 days) (Figure S1). No positive drug control was used in the MTT assay due to the lack of a reference first-line chemotherapeutic drug. In this regard, as reported in detail in Table 2, all thienoquinoline derivatives exhibited IC_{50} under 100 μM. The nitro compound **6b** resulted to be the most active, after both one and two doubling times, with IC_{50} in the micromolar range.

Table 2. Antiproliferative Activity of Compounds 6a−d against the TT(C634R) MTC Cell Line[a]

compound	3 days (IC_{50})	6 days (IC_{50})
6a	26.8 ± 2.7	24.3 ± 2.7
6b	3.6 ± 0.22	3.01 ± 0.035
6c	19.5 ± 9.1	11.7 ± 4.2
6d	73.2 ± 0.002	44.9 ± 5.2

[a]In the table, the antiproliferative activity is reported as IC_{50} ± SE (μM).

On the other hand, compound **6e** and the whole set of amino derivatives **7a−e** did not affect cancer cell growth appreciably, even at the highest concentration of 100 μM.

The capacity of anticancer drugs to influence cell cycle distribution can shed new light into the mechanism of their activity. Following cytotoxic evaluation, the effects of compounds **6a−d** were evaluated on cell cycle progression using the IC_{50} and the IC_{90} for each compound and an incubation time of approximately two doubling times (6 days). Following flow cytometry acquisition data were analyzed using ModFit software. TT cells treated with the thienoquinoline compounds showed no significant difference between the different cycle phases with respect to the untreated control (Figure 5). TT cells grew very slowly (the reported doubling time was approximately 83 h), so most of the cells were in the G1 phase of the cycle and few cells were in the G2/M phase. The compounds appear not to perturb the cycle phases.

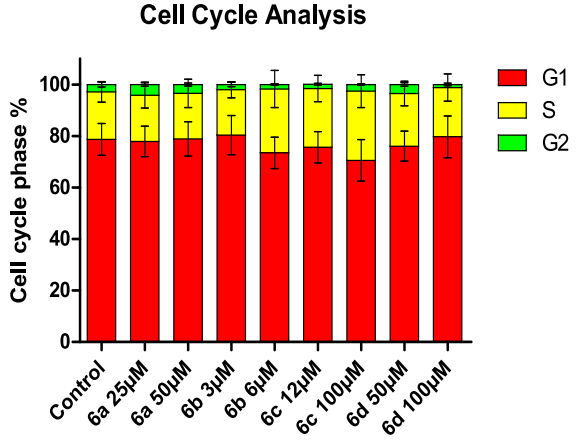

Figure 5. Cell cycle distribution of the TT cell line treated with compounds **6a−d** (at the IC_{50} and IC_{90}) as determined by flow cytometry. The data represent the mean ± SD of three experiments. The control represents the cells incubated with solvent only (DMSO).

The data represent the mean of three experiments. No significant difference between the cycle phases was determined in all drug treatments (Student's *t* test).

Apoptosis, a kind of programmed death, can be induced by common anticancer drug treatment. Fragmented DNA-containing nuclei could be detected as a hypodiploid large peak after staining with propidium iodide and measured by flow cytometry.[52] As shown Figure 6, the treatment of TT cells with different concentrations of the compounds for 6 days (two doubling times) increases the proportion of the cell in apoptosis in all concentrations tested but this does not reach statistical significance (Student's *t* test). Only compound **6c** at the IC_{90} (100 μM) gave a mean of 43.1 ± 6.2% of hypodiploid nuclei ($P < 0.05$ Student's *t* test).

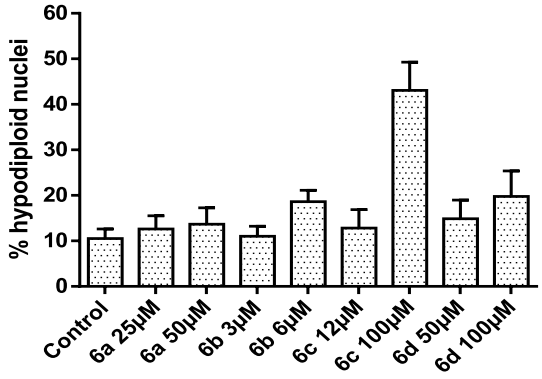

Figure 6. Apoptosis, as a percentage of hypodiploid nuclei determined by flow cytometry, of the TT cell line incubated with compounds **6a−d** at different concentrations (at the IC_{50} and IC_{90}) for two doubling times. The results are the mean ± SD of three experiments. The control represents the cells incubated with solvent only (DMSO).

Compounds **6a−d**, with the best antiproliferative activity, were further evaluated *in silico* by means of structure-based techniques. In detail, induced fit molecular docking (IFD) simulations were performed to gain insight into the possible binding mode and the pose of the identified anticancer agents into the RET tyrosine kinase domain.

Docking studies were performed using the X-ray structure of the RET ATP binding pocket (X-ray diffraction at a resolution of 1.87 Å; PDB code 6NEC).[14] As reference compounds, we used the MKI *nintedanib* and the *vandetanib*, a quinazoline RET inhibitor with structural similarity to the selected thienoquinoline compounds.

Table 3 shows the induced fit docking results (docking scores, prime energy, and IFD scores) of the identified thieno[3,2-*c*]quinoline molecules and the references (*nintedanib* and *vandetanib*) in complex with the RET tyrosine kinase domain.

Table 3. Prime Energy, Docking, and Induced Fit Docking (IFD) Scores of Derivatives 6a−d and Reference Compounds *Nintedanib* and *Vandetanib* in Complex with the RET ATP Binding Pocket (PDB Code 6NEC)

compound	docking score	prime energy	IFD score
6a	−9.529	−12678.36	−643.45
6b	−9.067	−12662.63	−642.20
6c	−8.863	−12676.47	−642.69
6d	−8.486	−12662.14	−641.59
nintedanib	−11.679	−12684.32	−645.89
vandetanib	−8.016	−12790.76	−647.55

Overall, compounds **6a−d** displayed IFD scores comparable with those of the two RET inhibitors. In addition, compounds

https://doi.org/10.1021/acsomega.3c03578
ACS Omega 2023, 8, 34640−34649

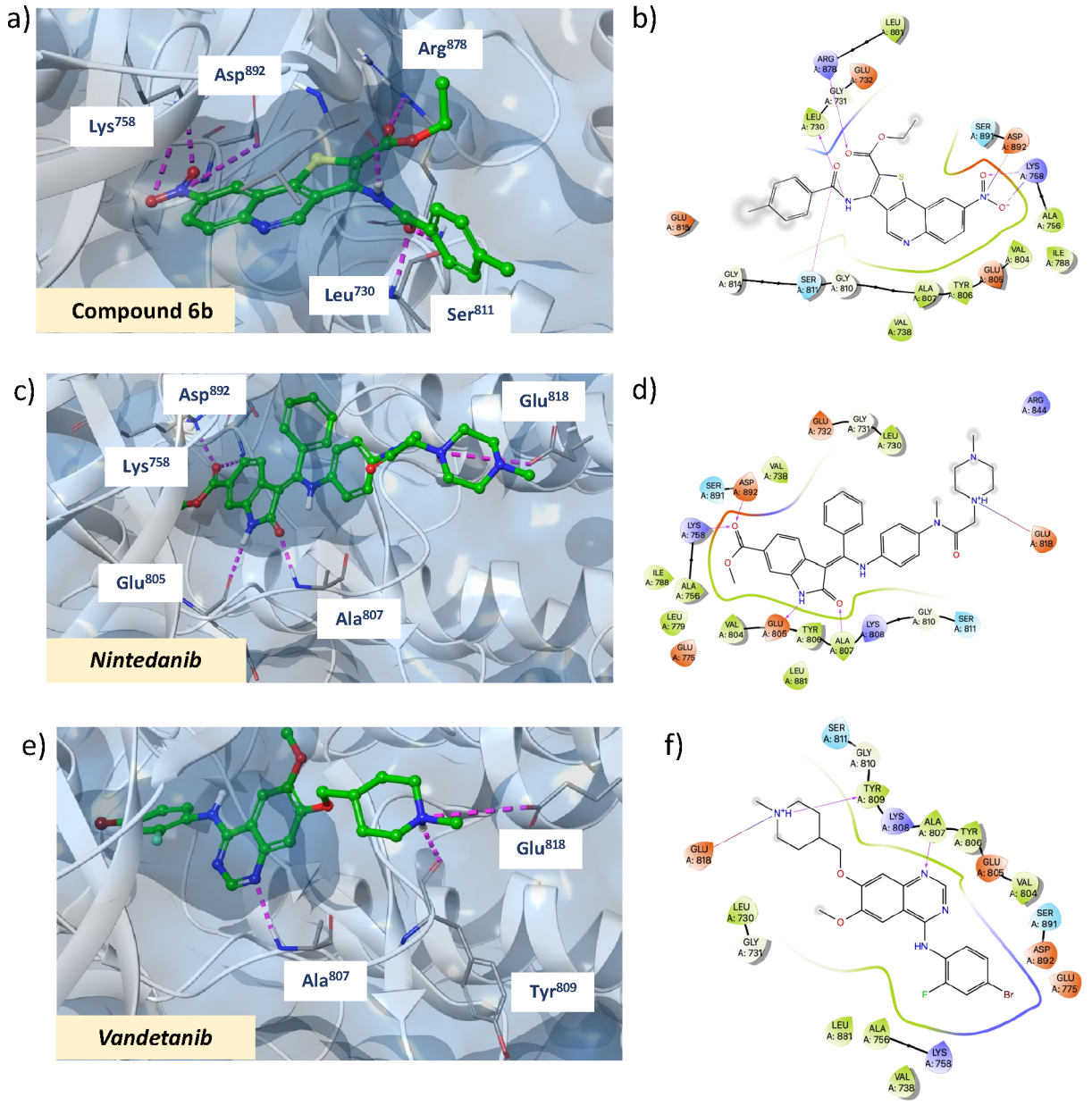

Figure 7. 3D view of the best docked pose and 2D ligand interaction diagram of **6b** (a, b), *nintedanib* (c, d), and *vandetanib* (e, f) in complex with the RET ATP binding pocket domain.

6a,b achieved higher docking scores than *vandetanib*, when the other parameters were analyzed.

A deep cross-analysis of the docked 3D complexes and of the key interactions formed by each compound with the protein binding site was performed (Figure 7a–f), and Table 4 provides an overview of the amino acids, located at a distance of 3 Å, involved in the binding with compounds **6a–d** and the two reference compounds.

All the selected derivatives formed a total number of interactions comparable to the already approved RET inhibitors (in the range of 16–20 vs 21 and 18 interactions for *nintedanib* and *vandetanib*, respectively), especially with key residues such as Leu^{730}, Gly^{731} Gly^{732}, Val^{738}, Ala^{756}, Lys^{758}, Ile^{788}, Val^{804} (gatekeeper residue), and Gly^{805} in the N-lobe; Tyr^{806}, Ala^{807}, Gly^{810}, and Ser^{811} in the crucial hinge region, which determines the access to the hydrophobic pocket; and Arg^{878}, Leu^{881}, Ser^{891}, and Asp^{892} in the C-lobe.

In addition, the ligand–protein complexes and the 2D interaction diagram of compound **6b** (the most active compound in the *in vitro* assays) shown in Figure 7a–f identify and analyze the 3D orientation and the best pose of the compound under study into the binding pocket compared to *nintedanib* and *vandetanib*.

As shown, the thieno[3,2-*c*]quinoline core of **6b** plays a key role in both the insertion into the ATP binding pocket of the RET kinase and in the formation of the most of the stabilizing interactions with the key residues reported in Table 4. In particular, the 8-NO_2 group is well accommodated in the outer space of the hydrophobic pocket and interacts with crucial residues (Lys^{758} and Asp^{892}). This trend is confirmed also for compounds **6a**, **6c**, and **6d**, which assumed a similar pose and orientation in the pocket and formed a very close pattern of interactions (3D ligand–protein complexes and ligand interaction diagrams are reported in Figure S2). On the

https://doi.org/10.1021/acsomega.3c03578
ACS Omega 2023, 8, 34640–34649

Table 4. Overview of the Amino Acids Involved in the Binding of the Selected Compounds 6a−d, *Vandetanib*, and *Nintedanib* in the ATP Binding Site of the RET Kinase at 3 Å Proximity

	RET tyrosine kinase domain																							
	N-lobe									hinge/linker region							C-lobe							
title	L730	G731	G732	G733	V738	A756	K758	E775	L779	I788	V804[a]	E805	Y806	A807	K808	Y809	G810	S811	G814	E818	R844	R878	L881	S891	D892	tot.
6a	X[b]	X	X			X	X[b]			X	X	X	X	X			X	X[b]				X[b]	X	X	X[c]X[b]	17
6b	X[b]	X	X		X	X	X[b]X[c]			X	X	X	X	X			X	X[b]	X	X		X[b]	X	X	X[c]	20
6c	X[b]	X	X	X	X	X	X[c]			X	X	X	X	X			X	X[b]	X	X		X	X	X	X[c]	20
6d	X[b]	X			X	X	X[c]			X	X	X	X	X			X	X[b]				X	X	X	X[b]	16
nintedanib	X	X	X		X	X	X[b]	X	X	X	X	X[b]	X	X[b]	X		X	X		X[c]	X		X	X	X[b]	21
vandetanib	X	X			X	X	X	X			X	X	X	X[b]	X	X[b]	X	X		X[c]			X	X	X	18

[a]Gatekeeper residue. [b]H-bonds. [c]Salt bridges.

other hand, from the comparison with the reference compounds, it emerged as the more hindered tricyclic thienoquinoline core could partially impede a deeper insertion and interaction with the inside hydrophobic pocket, which in turn is possible for more flexible structures of *nintedanib* and *vandetanib* (e.g., interactions with Glu[775] and Leu[779]). Furthermore, both the reference compounds possess charged and polar side chains (protonated cyclic amines) capable of forming H-bonds on the protein surface and directed toward the solvent-exposed area, where, instead, the carboxamide benzoyl moiety of compounds **6a−d** is projected. Probably, the introduction of more polar and hydrophilic portions in this part of the thienoquinoline molecules could be a starting point for a process of lead structure optimization aimed at improving the interactions with both the solvent and the polar protein surface.

3. CONCLUSIONS

Thyroid cancer represents one of the most aggressive endocrine malignances responsible for a high mortality rate. Its extraordinary capability to evade conventional chemotherapy is due to the frequently deregulated and uncontrolled activity of the RET protein, a kinase that promotes cell proliferation and survival and for which many gain-of-function point mutations have been identified in MTC cells. In this light, RET appears to be a crucial target for the development of new therapeutics that can be used in the treatment of this tumor.

In this work, the in-house *in silico* ligand-based BIOTARGET[finder] tool, implemented in the DRUDIT[online] platform, was employed to screen a large database of heterocyclic small molecules against the RET kinase, aiming at identifying new antiproliferative agents active against MTC cells. This virtual screening allowed to select compounds **6a−e** and **7a−e**, with the little explored thieno[3,2-*c*]quinoline core, as the most promising potential RET inhibitors, with predicted activity in the same range of the approved RET inhibitors *vandetanib* and *nintedanib*.

The identified derivatives were synthetized in optimal yields by following an appropriate multistep synthetic pathway and isolated with an appropriate purity for the antiproliferative biological assays. Indeed, the MTT assay was performed against the particularly aggressive MTC cell line TT, harboring the RET point mutation C634R. After treatment with the 10 thienoquinoline derivatives, encouraging IC_{50} in the micromolar range (3−45 μM) were measured for derivatives **6a−d**. Further biological evaluations showed as the identified compounds did not affect appreciably the cell cycle and the apoptosis pathways.

In addition, structure-based docking studies were performed on the X-ray structures of the RET kinase. The comprehensive analysis of the ligand−protein 3D complexes and of the interactions between the selected derivatives and the amino acids of the active site provided interesting insights into the possible binding mode and pose of the selected compounds, especially in comparison to known inhibitors.

In conclusion, this study provided an interesting new series of compounds with encouraging antiproliferative activity against MTC cells, which can be used as the starting point for the development of new more effective inhibitors, with increased solubility and binding capability.

https://doi.org/10.1021/acsomega.3c03578
ACS Omega 2023, 8, 34640−34649

■ ASSOCIATED CONTENT

Supporting Information

The Supporting Information is available free of charge at https://pubs.acs.org/doi/10.1021/acsomega.3c03578.

In silico ligand and structure-based protocols, methods for compound synthesis and analysis, *in vitro* procedures, and supplemental figures (PDF)

■ AUTHOR INFORMATION

Corresponding Author

Annamaria Martorana − *Dipartimento di Scienze e Tecnologie Biologiche Chimiche e Farmaceutiche, University of Palermo, 90128 Palermo, Italy;* orcid.org/0000-0002-9560-1882; Email: annamaria.martorana@unipa.it

Authors

Gabriele La Monica − *Dipartimento di Scienze e Tecnologie Biologiche Chimiche e Farmaceutiche, University of Palermo, 90128 Palermo, Italy;* orcid.org/0000-0001-6510-1943

Giuseppe Pizzolanti − *Dipartimento di Scienze e Tecnologie Biologiche Chimiche e Farmaceutiche, University of Palermo, 90128 Palermo, Italy*

Concetta Baiamonte − *Dipartimento di Scienze e Tecnologie Biologiche Chimiche e Farmaceutiche, University of Palermo, 90128 Palermo, Italy*

Alessia Bono − *Dipartimento di Scienze e Tecnologie Biologiche Chimiche e Farmaceutiche, University of Palermo, 90128 Palermo, Italy;* orcid.org/0000-0002-9283-4920

Federica Alamia − *Dipartimento di Scienze e Tecnologie Biologiche Chimiche e Farmaceutiche, University of Palermo, 90128 Palermo, Italy*

Francesco Mingoia − *Dipartimento di Scienze e Tecnologie Biologiche Chimiche e Farmaceutiche, University of Palermo, 90128 Palermo, Italy*

Antonino Lauria − *Dipartimento di Scienze e Tecnologie Biologiche Chimiche e Farmaceutiche, University of Palermo, 90128 Palermo, Italy;* orcid.org/0000-0002-5116-6815

Complete contact information is available at: https://pubs.acs.org/10.1021/acsomega.3c03578

Author Contributions

Conceptualization, G.L.M. and A.M.; methodology, G.L.M., G.P., C.B., and A.M.; software, G.L.M. and A.L.; validation, G.L.M., F.A., and A.M.; formal analysis, A.L. and F.M.; investigation, G.L.M., G.P., C.B., and A.M.; data curation, G.L.M. and A.M.; writing—original draft preparation, A.B., G.L.M., and A.M.; writing—review and editing, G.L.M and A.M.; visualization, A.L. and F.M.; supervision, A.M.; project administration, A.M. All authors have given approval to the final version of the manuscript.

Funding

This research was funded by MUR, PNRR-M4C2, ECS_00000022, and FFR2023.

Notes

The authors declare no competing financial interest.

■ ACKNOWLEDGMENTS

The authors would like to thank the "SiciliAn Micro-nanOTecH Research And Innovation CEnter ″SAMOTHRACE″ (MUR, PNRR-M4C2, ECS_00000022), spoke 3 - Università degli Studi di Palermo ″S2-COMMs - Micro and Nanotechnologies for Smart & Sustainable Communities". The graphical abstract was partly generated using Server Medical Art (https://smart.servier.com, accessed on 3 July 2023), provided by Server, licensed under a Creative Commons Attribution 3.0 unported license.

■ REFERENCES

(1) Prete, A.; Borges de Souza, P.; Censi, S.; Muzza, M.; Nucci, N.; Sponziello, M. Update on Fundamental Mechanisms of Thyroid Cancer. *Front. Endocrinol.* **2020**, *11*, 102.

(2) San Román Gil, M.; Pozas, J.; Molina-Cerrillo, J.; Gómez, J.; Pian, H.; Pozas, M.; Carrato, A.; Grande, E.; Alonso-Gordoa, T. Current and Future Role of Tyrosine Kinases Inhibition in Thyroid Cancer: From Biology to Therapy. *Int. J. Mol. Sci.* **2020**, *21*, 4951.

(3) Liu, X.; Hu, X.; Shen, T.; Li, Q.; Mooers, B. H. M.; Wu, J. RET kinase alterations in targeted cancer therapy. *Cancer Drug Resist.* **2020**, *3*, 472−481.

(4) Luzón-Toro, B.; Fernández, R. M.; Villalba-Benito, L.; Torroglosa, A.; Antiñolo, G.; Borrego, S. Influencers on Thyroid Cancer Onset: Molecular Genetic Basis. *Genes* **2019**, *10*, 913.

(5) Ibáñez, C. F. *Structure and physiology of the RET receptor tyrosine kinase.* Cold Spring Harb Perspect Biol 2013, *5* (2), DOI: 10.1101/cshperspect.a009134.

(6) De Falco, V.; Carlomagno, F.; Li, H. Y.; Santoro, M. The molecular basis for RET tyrosine-kinase inhibitors in thyroid cancer. *Best Pract. Res., Clin. Endocrinol. Metab.* **2017**, *31*, 307−318.

(7) Jia, C. C.; Chen, W.; Feng, Z. L.; Liu, Z. P. Recent developments of RET protein kinase inhibitors with diverse scaffolds as hinge binders. *Future Med. Chem.* **2021**, *13*, 45−62.

(8) Li, J.; Shang, G.; Chen, Y. J.; Brautigam, C. A.; Liou, J.; Zhang, X.; Bai, X. C. Cryo-EM analyses reveal the common mechanism and diversification in the activation of RET by different ligands. *Elife* **2019**, *8*, No. e47650.

(9) Mulligan, L. M. RET revisited: expanding the oncogenic portfolio. *Nat. Rev. Cancer* **2014**, *14*, 173−186.

(10) Kawai, K.; Takahashi, M. Intracellular RET signaling pathways activated by GDNF. *Cell Tissue Res.* **2020**, *382*, 113−123.

(11) Engelmann, D.; Koczan, D.; Ricken, P.; Rimpler, U.; Pahnke, J.; Li, Z.; Pützer, B. M. Transcriptome analysis in mouse tumors induced by Ret-MEN2/FMTC mutations reveals subtype-specific role in survival and interference with immune surveillance. *Endocr.-Relat. Cancer* **2009**, *16*, 211−224.

(12) Knowles, P. P.; Murray-Rust, J.; Kjaer, S.; Scott, R. P.; Hanrahan, S.; Santoro, M.; Ibáñez, C. F.; McDonald, N. Q. Structure and chemical inhibition of the RET tyrosine kinase domain. *J. Biol. Chem.* **2006**, *281*, 33577−33587.

(13) Blume-Jensen, P.; Hunter, T. Oncogenic kinase signalling. *Nature* **2001**, *411*, 355−365.

(14) Terzyan, S. S.; Shen, T.; Liu, X.; Huang, Q.; Teng, P.; Zhou, M.; Hilberg, F.; Cai, J.; Mooers, B. H. M.; Wu, J. Structural basis of resistance of mutant RET protein-tyrosine kinase to its inhibitors nintedanib and vandetanib. *J. Biol. Chem.* **2019**, *294*, 10428−10437.

(15) Hadoux, J.; Schlumberger, M. Chemotherapy and tyrosine-kinase inhibitors for medullary thyroid cancer. *Best Pract. Res., Clin. Endocrinol. Metab.* **2017**, *31*, 335−347.

(16) Okamoto, K.; Kodama, K.; Takase, K.; Sugi, N. H.; Yamamoto, Y.; Iwata, M.; Tsuruoka, A. Antitumor activities of the targeted multi-tyrosine kinase inhibitor lenvatinib (E7080) against RET gene fusion-driven tumor models. *Cancer Lett.* **2013**, *340*, 97−103.

(17) Fallahi, P.; Ferrari, S. M.; Santini, F.; Corrado, A.; Materazzi, G.; Ulisse, S.; Miccoli, P.; Antonelli, A. Sorafenib and thyroid cancer. *BioDrugs* **2013**, *27*, 615−628.

(18) Borrello, M. G.; Ardini, E.; Locati, L. D.; Greco, A.; Licitra, L.; Pierotti, M. A. RET inhibition: implications in cancer therapy. *Expert Opin. Ther. Targets* **2013**, *17*, 403−419.

(19) Saha, D.; Ryan, K. R.; Lakkaniga, N. R.; Acharya, B.; Garcia, N. G.; Smith, E. L.; Frett, B. Targeting Rearranged during Transfection

in Cancer: A Perspective on Small-Molecule Inhibitors and Their Clinical Development. *J. Med. Chem.* **2021**, *64*, 11747−11773.
(20) Ayala-Aguilera, C. C.; Valero, T.; Lorente-Macías, Á.; Baillache, D. J.; Croke, S.; Unciti-Broceta, A. Small Molecule Kinase Inhibitor Drugs (1995-2021): Medical Indication, Pharmacology, and Synthesis. *J. Med. Chem.* **2022**, *65*, 1047−1131.
(21) Hu, X.; Khatri, U.; Shen, T.; Wu, J. Progress and challenges in RET-targeted cancer therapy. *Front. Med.* **2023**, *17*, 207−219.
(22) Shen, T.; Hu, X.; Liu, X.; Subbiah, V.; Mooers, B. H. M.; Wu, J. The L730V/I RET roof mutations display different activities toward pralsetinib and selpercatinib. *NPJ Precis. Oncol.* **2021**, *5*, 48.
(23) Moccia, M.; Yang, D.; Lakkaniga, N. R.; Frett, B.; McConnell, N.; Zhang, L.; Brescia, A.; Federico, G.; Salerno, P.; Santoro, M.; Li, H.-y.; Carlomagno, F. Targeted activity of the small molecule kinase inhibitor Pz-1 towards RET and TRK kinases. *Sci. Rep.* **2021**, *11*, 16103.
(24) Dinér, P.; Alao, J. P.; Söderlund, J.; Sunnerhagen, P.; Grøtli, M. Preparation of 3-substituted-1-isopropyl-1H-pyrazolo[3,4-d]-pyrimidin-4-amines as RET kinase inhibitors. *J. Med. Chem.* **2012**, *55*, 4872−4876.
(25) Yoon, H.; Shin, I.; Nam, Y.; Kim, N. D.; Lee, K. B.; Sim, T. Identification of a novel 5-amino-3-(5-cyclopropylisoxazol-3-yl)-1-isopropyl-1H-pyrazole-4-carboxamide as a specific RET kinase inhibitor. *Eur. J. Med. Chem.* **2017**, *125*, 1145−1155.
(26) Mathison, C. J. N.; Chianelli, D.; Rucker, P. V.; Nelson, J.; Roland, J.; Huang, Z.; Yang, Y.; Jiang, J.; Xie, Y. F.; Epple, R.; et al. Efficacy and Tolerability of Pyrazolo[1,5-a]pyrimidine RET Kinase Inhibitors for the Treatment of Lung Adenocarcinoma. *ACS Med. Chem. Lett.* **2020**, *11*, 558−565.
(27) Yoon, H.; Kwak, Y.; Choi, S.; Cho, H.; Kim, N. D.; Sim, T. A Pyrazolo[3,4-d]pyrimidin-4-amine Derivative Containing an Isoxazole Moiety Is a Selective and Potent Inhibitor of RET Gatekeeper Mutants. *J. Med. Chem.* **2016**, *59*, 358−373.
(28) Wang, C.; Liu, H.; Song, Z.; Ji, Y.; Xing, L.; Peng, X.; Wang, X.; Ai, J.; Geng, M.; Zhang, A. Synthesis and structure-activity relationship study of pyrazolo[3,4-d]pyrimidines as tyrosine kinase RET inhibitors. *Bioorg. Med. Chem. Lett.* **2017**, *27*, 2544−2548.
(29) Newton, R.; Bowler, K. A.; Burns, E. M.; Chapman, P. J.; Fairweather, E. E.; Fritzl, S. J. R.; Goldberg, K. M.; Hamilton, N. M.; Holt, S. V.; Hopkins, G. V.; et al. The discovery of 2-substituted phenol quinazolines as potent RET kinase inhibitors with improved KDR selectivity. *Eur. J. Med. Chem.* **2016**, *112*, 20−32.
(30) Jordan, A. M.; Begum, H.; Fairweather, E.; Fritzl, S.; Goldberg, K.; Hopkins, G. V.; Hamilton, N. M.; Lyons, A. J.; March, H. N.; Newton, R.; et al. Anilinoquinazoline inhibitors of the RET kinase domain-Elaboration of the 7-position. *Bioorg. Med. Chem. Lett.* **2016**, *26*, 2724−2729.
(31) Rowbottom, M. W.; Faraoni, R.; Chao, Q.; Campbell, B. T.; Lai, A. G.; Setti, E.; Ezawa, M.; Sprankle, K. G.; Abraham, S.; Tran, L.; et al. Identification of 1-(3-(6,7-dimethoxyquinazolin-4-yloxy)-phenyl)-3-(5-(1,1,1-trifluoro-2-methylpropan-2-yl)isoxazol-3-yl)urea hydrochloride (CEP-32496), a highly potent and orally efficacious inhibitor of V-RAF murine sarcoma viral oncogene homologue B1 (BRAF) V600E. *J. Med. Chem.* **2012**, *55*, 1082−1105.
(32) Drilon, A.; Fu, S.; Patel, M. R.; Fakih, M.; Wang, D.; Olszanski, A. J.; Morgensztern, D.; Liu, S. V.; Cho, B. C.; Bazhenova, L.; et al. A Phase I/Ib Trial of the VEGFR-Sparing Multikinase RET Inhibitor RXDX-105. *Cancer Discov.* **2019**, *9*, 384−395.
(33) Li, G. G.; Somwar, R.; Joseph, J.; Smith, R. S.; Hayashi, T.; Martin, L.; Franovic, A.; Schairer, A.; Martin, E.; Riely, G. J. Antitumor Activity of RXDX-105 in Multiple Cancer Types with *RET* Rearrangements or Mutations. *Clin. Cancer Res.* **2017**, *23*, 2981−2990.
(34) Mologni, L.; Rostagno, R.; Brussolo, S.; Knowles, P. P.; Kjaer, S.; Murray-Rust, J.; Rosso, E.; Zambon, A.; Scapozza, L.; McDonald, N. Q.; et al. Synthesis, structure-activity relationship and crystallographic studies of 3-substituted indolin-2-one RET inhibitors. *Bioorg. Med. Chem.* **2010**, *18*, 1482−1496.
(35) Brandt, W.; Mologni, L.; Preu, L.; Lemcke, T.; Gambacorti-Passerini, C.; Kunick, C. Inhibitors of the RET tyrosine kinase based on a 2-(alkylsulfanyl)-4-(3-thienyl)nicotinonitrile scaffold. *Eur. J. Med. Chem.* **2010**, *45*, 2919−2927.
(36) Schenck Eidam, H.; Russell, J.; Raha, K.; DeMartino, M.; Qin, D.; Guan, H. A.; Zhang, Z.; Zhen, G.; Yu, H.; Wu, C.; et al. Discovery of a First-in-Class Gut-Restricted RET Kinase Inhibitor as a Clinical Candidate for the Treatment of IBS. *ACS Med. Chem. Lett.* **2018**, *9*, 623−628.
(37) La Pietra, V.; Sartini, S.; Botta, L.; Antonelli, A.; Ferrari, S. M.; Fallahi, P.; Moriconi, A.; Coviello, V.; Quattrini, L.; Ke, Y. Y.; et al. Challenging clinically unresponsive medullary thyroid cancer: Discovery and pharmacological activity of novel RET inhibitors. *Eur. J. Med. Chem.* **2018**, *150*, 491−505.
(38) Lauria, A.; Martorana, A.; La Monica, G.; Mannino, S.; Mannino, G.; Peri, D.; Gentile, C. In Silico Identification of Small Molecules as New Cdc25 Inhibitors through the Correlation between Chemosensitivity and Protein Expression Pattern. *Int. J. Mol. Sci.* **2021**, *22*, 3714.
(39) La Monica, G.; Lauria, A.; Bono, A.; Martorana, A. Off-target-based design of selective hiv-1 protease inhibitors. *Int. J. Mol. Sci.* **2021**, *22*, 6070.
(40) Martorana, A.; La Monica, G.; Bono, A.; Mannino, S.; Buscemi, S.; Palumbo Piccionello, A.; Gentile, C.; Lauria, A.; Peri, D. Antiproliferative Activity Predictor: A New Reliable In Silico Tool for Drug Response Prediction against NCI60 Panel. *Int. J. Mol. Sci.* **2022**, *23*, 14374.
(41) Lauria, A.; Patella, C.; Abbate, I.; Martorana, A.; Almerico, A. M. Lead optimization through VLAK protocol: new annelated pyrrolo-pyrimidine derivatives as antitumor agents. *Eur. J. Med. Chem.* **2012**, *55*, 375−383.
(42) Lauria, A.; Abbate, I.; Patella, C.; Martorana, A.; Dattolo, G.; Almerico, A. M. New annelated thieno[2,3-e][1,2,3]triazolo[1,5-a]pyrimidines, with potent anticancer activity, designed through VLAK protocol. *Eur. J. Med. Chem.* **2013**, *62*, 416−424.
(43) Lauria, A.; Tutone, M.; Barone, G.; Almerico, A. M. Multivariate analysis in the identification of biological targets for designed molecular structures: the BIOTA protocol. *Eur. J. Med. Chem.* **2014**, *75*, 106−110.
(44) Lauria, A.; Abbate, I.; Gentile, C.; Angileri, F.; Martorana, A.; Almerico, A. M. Synthesis and biological activities of a new class of heat shock protein 90 inhibitors, designed by energy-based pharmacophore virtual screening. *J. Med. Chem.* **2013**, *56*, 3424−3428.
(45) Martorana, A.; Lauria, A. Design of antitumor drugs targeting c-kit receptor by a new mixed ligand-structure based method. *J. Mol. Graphics Modell.* **2020**, *100*, No. 107666.
(46) Lauria, A.; Mannino, S.; Gentile, C.; Mannino, G.; Martorana, A.; Peri, D. DRUDIT: web-based DRUgs DIscovery Tools to design small molecules as modulators of biological targets. *Bioinformatics* **2020**, *36*, 1562−1569.
(47) Martorana, A.; La Monica, G.; Lauria, A. Quinoline-Based Molecules Targeting c-Met, EGF, and VEGF Receptors and the Proteins Involved in Related Carcinogenic Pathways. *Molecules* **2020**, *25*, 4279.
(48) Lauria, A.; La Monica, G.; Bono, A.; Martorana, A. Quinoline anticancer agents active on DNA and DNA-interacting proteins: From classical to emerging therapeutic targets. *Eur. J. Med. Chem.* **2021**, *220*, No. 113555.
(49) Zschäbitz, S.; Grüllich, C. Lenvantinib: A Tyrosine Kinase Inhibitor of VEGFR 1-3, FGFR 1-4, PDGFRα, KIT and RET. *Recent Results Cancer Res.* **2018**, *211*, 187−198.
(50) Roskoski, R., Jr; Sadeghi-Nejad, A. Role of RET protein-tyrosine kinase inhibitors in the treatment RET-driven thyroid and lung cancers. *Pharmacol. Res.* **2018**, *128*, 1−17.
(51) Wissner, A.; Overbeek, E.; Reich, M. F.; Floyd, M. B.; Johnson, B. D.; Mamuya, N.; Rosfjord, E. C.; Discafani, C.; Davis, R.; Shi, X.; Rabindran, S. K.; Gruber, B. C.; Ye, F.; Hallett, W. A.; Nilakantan, R.; Shen, R.; Wang, Y. F.; Greenberger, L. M.; Tsou, H. R. Synthesis and

https://doi.org/10.1021/acsomega.3c03578
ACS Omega 2023, 8, 34640−34649

structure-activity relationships of 6,7-disubstituted 4-anilinoquinoline-3-carbonitriles. The design of an orally active, irreversible inhibitor of the tyrosine kinase activity of the epidermal growth factor receptor (EGFR) and the human epidermal growth factor receptor-2 (HER-2). *J. Med. Chem.* **2003**, *46*, 49−63.

(52) Riccardi, C.; Nicoletti, I. Analysis of apoptosis by propidium iodide staining and flow cytometry. *Nat. Protoc.* **2006**, *1*, 1458−1461.

https://doi.org/10.1021/acsomega.3c03578
ACS Omega 2023, 8, 34640−34649